PAPER

Investigation of the reabsorption effect in an all-fiberized mode-locked thulium-doped fibre laser

IOP Publishing | Astro Ltd Laser Physics

Laser Phys. **29** (2019) 045104 (5pp) https://doi.org/10.1088/1555-6611/aaffc5

Investigation of the reabsorption effect in an all-fiberized mode-locked thulium-doped fibre laser

Baofu Zhang[1], Xionghua Zheng[1], Jing Guo[2], Zhongxing Jiao[1] and Biao Wang[1,2]

[1] School of Physics, Sun Yat-sen University, Guangzhou 510275, People's Republic of China

[2] Sino-French Institute of Nuclear Engineering and Technology, Sun Yat-sen University, Guangzhou 510275, People's Republic of China

E-mail: jiaozhx@mail.sysu.edu.cn and wangbiao@mail.sysu.edu.cn

Received 30 August 2018, revised 28 December 2018
Accepted for publication 28 December 2018
Published 12 March 2019

Abstract

We investigate the influence of the reabsorption effect on pulse characteristics in an all-fiberized ultra-fast thulium-doped fibre laser system. Mode-locked operation was enabled by a semiconductor saturable absorber mirror, and the laser generated stable ultra-short pulses at a repetition rate of 11.29 MHz. By changing the length of the thulium-doped fibre, and hence the reabsorption loss, we found that the reabsorption effect had a significant influence on the optical spectrum and pulse duration of the mode-locked fibre laser. Output durations from 2.04 ps to 20.8 ps have been achieved, corresponding to operating wavelengths changing from 1968.9 nm to 2054.7 nm. Qualitative explanations of these phenomena have also been demonstrated.

Keywords: thulium-doped fibre laser, all-fiberized, mode-locked, reabsorption effect

(Some figures may appear in colour only in the online journal)

1. Introduction

Mode-locked laser systems of the 2 μm region have received widespread application interest in recent years due to their capabilities for producing pulses with energy above the nJ regime and duration down to the fs regime. Among these laser systems, mode-locked thulium-doped fibre lasers (MLTDFLs) with an all-fibre configuration offer superior properties compared to other solid-state lasers, including compact construction, high spatial mode quality, and enhanced thermal management. Therefore, they are considered to be significant candidates for the generation of ultra-short 2 μm pulses with practical applications in micromachining [1], surgery [2, 3], remote environmental sensing [4], and wavelength conversion to ultra-fast mid-infrared lasers [5–7].

To meet the requirements of different applications, simple MLTDFL designs, which can produce ultra-fast 2 μm lasers with suitable pulse characteristics, are demanded. Because of the high peak power in the fibre cavity, the characteristics of output pulses, such as pulse duration, can be significantly influenced by several cavity parameters of the MLTDFL. These parameters include the overall cavity dispersion, the gain and loss of laser cavity, and the spectral filters, which have been investigated systematically through theoretical models and experiments [8–11].

The laser reabsorption effect of the thulium-doped fibre is a well-known phenomenon and has been demonstrated in several thulium-doped fibre lasers (TDFL) designs [12, 13]. Due to the three-level nature of the thulium ion, reabsorption loss depends on the lasing wavelength and inversion level (and hence the length of the thulium-doped fibre). The output wavelength of the TDFL can be selected in the range 1870–2000 nm by selection of the appropriate thulium-doped fibre length, which has been reported by Clarkson *et al* [13]. Moreover, because the intrinsic emission peak of the thulium-doped fibre is close to 1900 nm [14], the reabsorption effect may have influences on not only the lasing wavelength but also its bandwidth. Therefore, the output duration of a MLTDFL

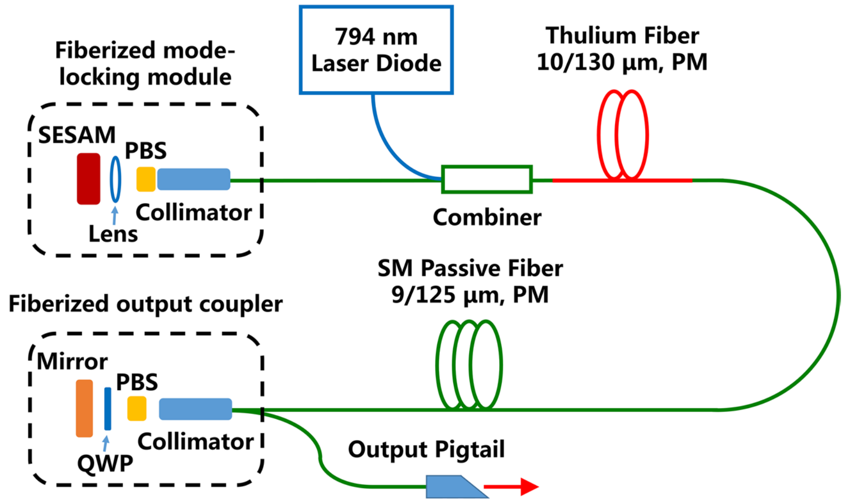

Figure 1. The scheme of the all-fiberized mode-locked thulium-doped fibre laser. SESAM, semiconductor saturable absorber mirror; PBS, polarizing beam splitter; PM, polarization maintaining; QWP, quarter wave plate; SM, single mode.

may be influenced by the reabsorption effect. However, little attention has been paid to the study of the reabsorption effect in MLTDFLs.

In this paper, we investigate the influence of the reabsorption effect in an all-fiberized polarized MLTDFL design. With mode-locked operation enabled by a semiconductor saturable absorber mirror (SESAM), the TDFL produces self-starting ultra-short pulses with linear polarization. By employing the reabsorption effect and changing the length of thulium-doped fibre, the duration of the output pulses can be changed from 2.04 ps to 20.8 ps, corresponding to operating central wavelengths from 1968.9 nm to 2054.7 nm.

2. Experimental setup

A schematic of our MLTDFL system is depicted in figure 1; the experimental setup is similar to that presented in our previous work [15]. The laser was arranged in an all-fiberized linear resonator configuration, and its pump source was a commercial continuous-wave (CW) laser diode operating at 794 nm. The pump laser was coupled into the laser cavity through a fibre combiner whose signal fibre and output fibre have a double-clad polarization-maintaining (PM) structure with a core diameter of 10 μm and a cladding diameter of 130 μm (10/130 μm). The pump transmission efficiency of the combiner was measured to be 92%, and its signal insertion loss was about 0.05 dB.

As shown in figure 1, the laser cavity consisted of two fiberized modules, which acted as the mode-locking element and the output coupler (OC), respectively. A fibre collimator, a polarizing beam splitter (PBS), a focusing lens, and a $4 \times 4\,\text{mm}^2$ SESAM (BATOP GmbH) were embedded in the fiberized mode-locking module, which was spliced to the signal port of the combiner. The SESAM has a high reflection band from 1900 nm to 2080 nm, with a relaxation time constant of 10 ps and modulation depth of 18%. Moreover, the spot size on the SESAM was designed to be 100 μm diameter to ensure sufficient saturation fluence and avoid optical damage. The fiberized OC module consisted of a fibre collimator, a PBS, a quarter wave plate, and a monochrome mirror. It was constructed with a special double-fibre-pigtail configuration, and it has a reflectivity of 90% at laser wavelength (1900–2080 nm). The transmission port of the OC module was spliced to a coated 8-degree-cleaved output pigtail with high transmittance ($T > 99.9\%$) at laser wavelength. The insertion losses of the mode-locking module and the OC module were measured to be 1 dB and 1.2 dB, respectively. In addition, PBSs used in both modules introduced high loss for the light with its polarization in the fast-axis direction of the PM fibre, and ensured the single polarization operation of the laser.

A segment of PM thulium-doped fibre (Nufern Inc.), with the same structure as the output fibre of the combiner (10/130 μm), was utilized as the gain medium. To investigate the output laser characteristics with the reabsorption filter effect, the length of thulium-doped fibre was reduced stepwise from 2.1 m to 1.1 m in our experiments. A segment of single-mode (SM) PM passive fibre was spliced to the thulium-doped fibre; its length was adjusted according to the length of thulium-doped fibre to ensure that the total cavity length was close to 8.85 m at each step. Moreover, part of this single-clad fibre acted as a residual cladding pump striper for the purpose of achieving stable mode-locked pulses. Except for the fibre pigtails of the combiner, all the passive fibres mentioned above have an SM PM 9/125 μm (core/cladding) structure. In addition, anomalous dispersions of the thulium-doped fibre and the passive fibre used in the TDFL system were estimated to be $-76\,\text{ps}^2\,\text{km}^{-1}$ and $-67\,\text{ps}^2\,\text{km}^{-1}$ at laser wavelength, respectively. Neglecting the small amount of dispersion introduced by the free-space components, the net dispersion of the cavity was calculated to be between $-0.5851\,\text{ps}^2$ and $-0.5761\,\text{ps}^2$ with different lengths of thulium-doped fibre. Without any active cooling condition, the whole laser cavity was mounted on an aluminium heat sink at room temperature.

3. Results and discussion

The performance of the laser system was achieved using a power meter (Newport, 1917-R), a 2 GHz digital phosphor

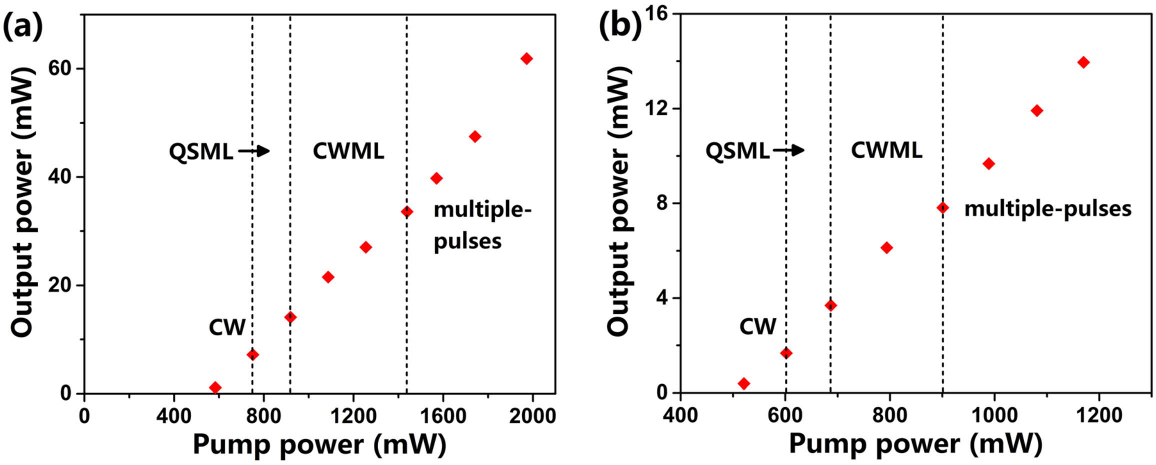

Figure 2. The average output power with varying pump power when the active fibre length was (a) 2.1 m and (b) 1.1 m. CW, continuous-wave; QSML, Q-switched mode-locking; CWML, continuous-wave mode-locking.

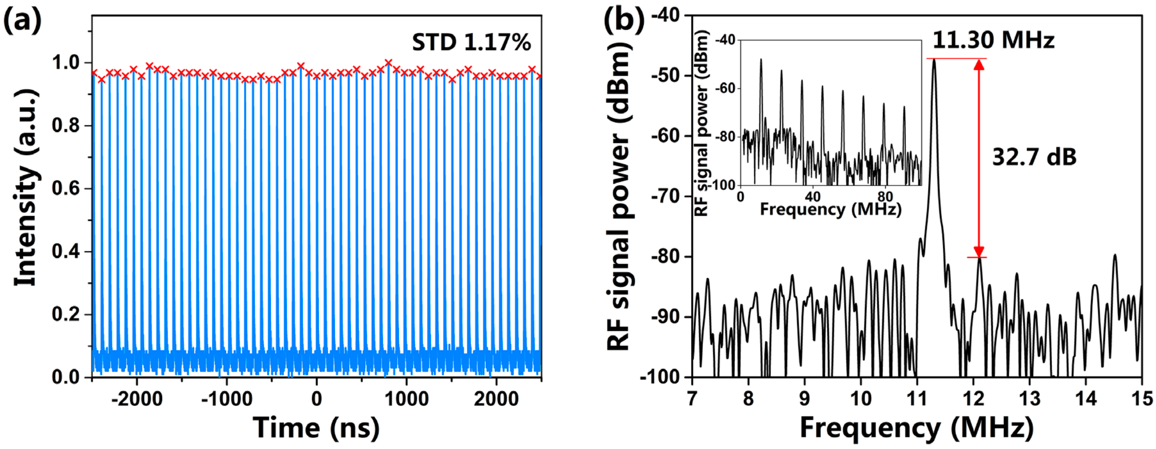

Figure 3. (a) The pulse trace, and (b) the RF spectrum of the laser when the active fibre length was 1.1 m. Inset of (b) the wide span RF spectrum. STD, standard deviation.

oscilloscope (Tektronix, DPO5204B) coupled with an InGaAs photodetector (Thorlabs, DET10D/M), a radio frequency (RF) spectrum analyser (Tektronix, RSA306B) coupled with the same InGaAs photodetector, an optical spectrum analyser (HORIBA, iHR550), a home-made autocorrelator, and a home-made polarization analyser.

Figure 2 illustrates the average output power of the laser versus the input pump power, corresponding to the active fibre lengths of 2.1 m and 1.1 m. For the length of thulium-doped fibre between 2.1 m and 1.1 m, the lasing thresholds of the laser were different due to the variation in gain and reabsorption loss in the laser cavity. For example, as shown in figure 2, the threshold of the laser was 583.6 mW when the active fibre length was 2.1 m, and it was slightly lower (521.0 mW) when the active fibre length was 1.1 m. However, the laser with different lengths of thulium-doped fibre had similar pulse train performance. At first, the laser operated in the CW regime when its threshold was reached. After the pump power was increased slightly, the laser then began to operate in the Q-switched mode-locking regime, whereas at slightly higher pump power it entered a self-starting single-pulse operation called the CW mode-locking (CWML) regime. When the pump power reached a higher level, the laser exhibited a complex multiple-pulse operation dynamic. Figure 3 illustrates a typical pulse train, and the RF spectrum of the laser when the active fibre length was 1.1 m. As shown in figure 3(a), in the CWML regime (which we focus on in this paper), the MLTDFL produced a stable pulse train with a small pulse-to-pulse intensity fluctuation less than 1.2% (standard deviation) in the 500 ns per division timescale. Figure 3(b) shows the RF spectrum recorded in the CWML regime, centred at the frequency of 11.30 MHz; it indicates that the laser emitted pulse trains with a repetition rate of 11.30 MHz, corresponding to the cavity length of 8.85 m. The RF spectrum in a wide-scan measurement is depicted in the inset of figure 3(b), which further confirms stable single-pulse operation of the laser because no signals from multi-pulsing or harmonic mode-locking can be found in the spectrum [16]. The signal to noise ratio of the RF spectrum seems to be low (32.7 dB), since only weak scattering power was used for detecting and the photodetector had a long rise time of about 10 ns.

Ascribed to the reabsorption effect and no additional spectral filter in the cavity, the spectrum of the laser was significantly influenced by the length of thulium-doped fibre. Figures 4(a) and (b) illustrate two spectra of ultra-short pulses generated by MLTDFLs, corresponding to the active fibre lengths of 2.1 m

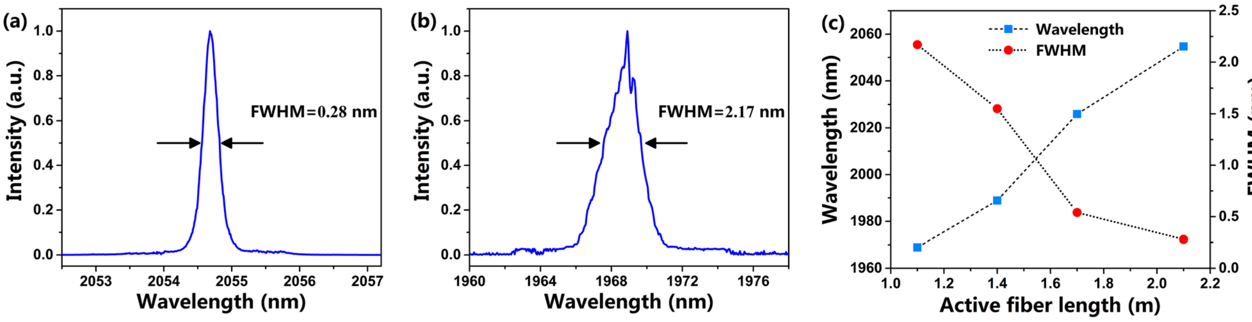

Figure 4. The spectra of the laser with the active fibre lengths of (a) 2.1 m (central wavelength of 2054.7 nm) and (b) 1.1 m (central wavelength of 1968.9 nm). (c) The central wavelength and the FWHM of the laser with varying active fibre length.

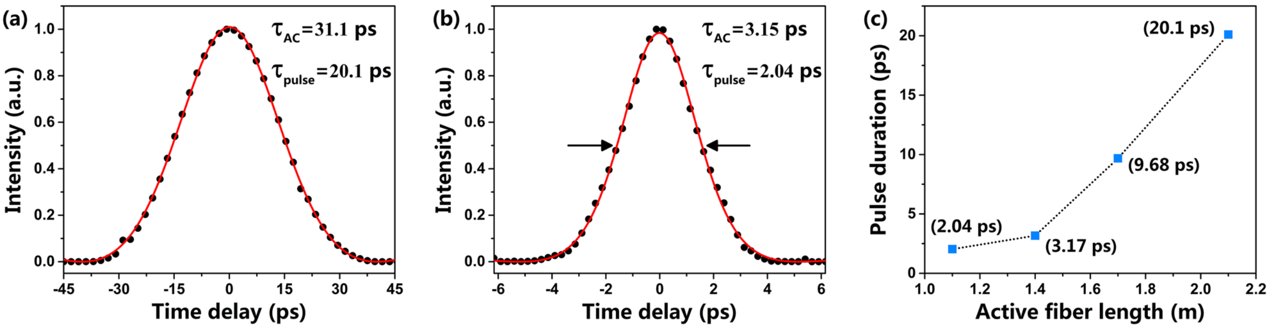

Figure 5. The autocorrelation traces of the laser with the active fibre lengths of (a) 2.1 m and (b) 1.1 m. (c) The output pulse duration with varying active fibre length. AC, autocorrelation.

and 1.1 m. For the length of thulium-doped fibre reduced stepwise from 2.1 m to 1.1 m, the development of the laser spectra is shown in figure 4(c); all these spectra were obtained when the laser operated in the stable single-pulse regime. As shown in figure 4, there is a noticeable shift of the spectrum centre towards shorter wavelengths (from 2054.7 nm to 1968.9 nm) with the decrease in the active fibre length. This phenomenon indicates that longer thulium-doped fibre introduces more reabsorption losses at shorter wavelengths in our laser cavity, and it is in good agreement with the physical mechanism of the reabsorption effect mentioned above and presented in [12, 13]. Moreover, as the active fibre length decreased (and hence the operating spectrum centre shifted towards a shorter wavelength), the spectrum bandwidth (full width at half maximum, FWHM) of the laser was considerably broadened at an order of magnitude from 0.28 nm to 2.17 nm. The broadening bandwidth was probably caused by the fact that the intrinsic emission peak of the thulium-doped fibre used in our laser is close to 1900 nm, and thus more adjacent modes were able to lase at shorter wavelengths in our case.

Figures 5(a) and (b) illustrate two autocorrelation traces of ultra-short pulses generated by the laser, corresponding to the spectra mentioned above with the active fibre lengths of 2.1 m and 1.1 m. By assuming a hyperbolic-secant pulse shape, which is typical for optical solitons, the measured autocorrelation widths of 32.1 ps and 3.15 ps correspond to pulse durations of 20.8 ps and 2.04 ps, respectively. Since the relaxation time constant of the SESAM is 10 ps, the pulse duration suggested that the SESAM could act as either a fast saturable absorber or a slow saturable absorber in our laser system. In addition, with the spectrum bandwidths of 0.28 nm and 2.17 nm, the time-bandwidth products were calculated to be 0.414 and 0.343, respectively. Both output pulses were slightly chirped compared to the transform-limit value of 0.315 for the hyperbolic-secant pulse. The output pulse duration of the laser with varying active fibre length is depicted in figure 5(c): pulse durations of the MLTDFLs became longer as the active fibre length increased. As mentioned above, the reabsorption effect has influences on the lasing spectrum. Therefore, the phenomenon shown in figure 5(c) can be qualitatively explained by the relationship between the spectrum and duration of a mode-locked laser when it operates in the soliton regime [17]. These results indicate that the reabsorption effect can have significant influences on the output duration of the MLTDFL.

The output polarization extinction ratios (PERs) of the laser with different lengths of thulium-doped fibre were also measured. When the laser operated in the stable single-pulse regime, PERs of >27 dB were recorded, indicating that the output beams were more than 99.8% linearly polarized in all situations. The mild depolarization was probably caused by the misalignments of the fiberized modules in the fabrication process or thermal effects introduced by high intracavity power.

4. Conclusions

In summary, we have investigated the influence of the reabsorption effect in an all-fiberized MLTDFL system. Mode-locked by a SESAM, the laser system was self-starting and generated stable CWML pulses at a repetition rate of 11.30 MHz. By changing the length of thulium-doped fibre, and hence the reabsorption loss, we found that the reabsorption had significant influences on the pulse characteristics of the MLTDFL, including the output spectrum, bandwidth, and duration. An output pulse duration from 2.04 ps to 20.8 ps was achieved, corresponding to central wavelengths from 1968.9 nm to 2054.7 nm. However, based on the reabsorption effect, the pulse duration and the spectrum of the MLTDFL will be changed simultaneously, which may be a limitation in some applications. Future work will focus on the numerical model of the reabsorption effect in the MLTDFL system to provide additional insight into the physics of those phenomena.

Acknowledgments

This work was supported in part by the National Natural Science Foundation of China under Grant Nos. 61308056 and 11204044, and the Natural Science Foundation of Guangdong, China, under Grant Nos. 2017A030310305 and 2018A030310092. The authors would like to acknowledge Advanced Fiber Resources (Zhuhai) Ltd for the technical support in this work. Special thanks go to Deping Zhao, Jiannan Lu, Haiming Li, Yi Xu, Wenfu Liang, and Changbin Xie for their helpful guidance in fiberized device design and fabrication.

References

[1] Gattass R R and Mazur E 2008 Femtosecond laser micromachining in transparent materials *Nat. Photon.* **2** 219–25
[2] Fried N M and Murray K E 2005 High-power thulium fiber laser ablation of urinary tissues at 1.94 μm *J. Endourol.* **19** 25–31
[3] Fried N M 2005 High-power laser vaporization of the canine prostate using a 110 W Thulium fiber laser at 1.91 μm *Lasers Surg. Med.* **36** 52–6
[4] Zeller W, Naehle L, Fuchs P, Gerschuetz F, Hildebrandt L and Koeth J 2010 DFB lasers between 760 nm and 16 μm for sensing applications *Sensors* **10** 2492–10
[5] Leindecker N, Marandi A, Byer R L, Vodopyanov K L, Jiang J, Hartl I, Fermann M and Schunemann P G 2012 Octave-spanning ultrafast OPO with 2.6–6.1 μm instantaneous bandwidth pumped by femtosecond Tm-fiber laser *Opt. Express* **20** 7046–53
[6] Granzow N, Schmidt M, Chang W, Wang L, Coulombier Q, Troles J, Toupin P, Hartl I, Lee K and Fermann M 2013 Mid-infrared supercontinuum generation in As_2S_3-silica 'nano-spike' step-index waveguide *Opt. Express* **21** 10969–77
[7] Phillips C, Jiang J, Mohr C, Lin A, Langrock C, Snure M, Bliss D, Zhu M, Hartl I and Harris J 2012 Widely tunable midinfrared difference frequency generation in orientation-patterned GaAs pumped with a femtosecond Tm-fiber system *Opt. Lett.* **37** 2928–30
[8] Haxsen F, Wandt D, Morgner U, Neumann J and Kracht D 2010 Pulse characteristics of a passively mode-locked thulium fiber laser with positive and negative cavity dispersion *Opt. Express* **18** 18981–8
[9] Sobon G, Sotor J, Martynkien T and Abramski K M 2016 Ultra-broadband dissipative soliton and noise-like pulse generation from a normal dispersion mode-locked Tm-doped all-fiber laser *Opt. Express* **24** 6156–61
[10] Tang Y, Chong A and Frank W W 2015 Generation of 8 nJ pulses from a normal-dispersion thulium fiber laser *Opt. Lett.* **40** 2361–4
[11] Mashiko Y, Fujita E and Tokurakawa M 2016 Tunable noise-like pulse generation in modelocked Tm fiber laser with a SESAM *Opt. Express* **24** 26515–20
[12] Jackson S D and King T A 1998 High-power diode-cladding-pumped Tm-doped silica fiber laser *Opt. Lett.* **23** 1462–4
[13] Clarkson W A, Barnes N P, Turner P W, Nilsson J and Hanna D C 2002 High-power cladding-pumped Tm-doped silica fiber laser with wavelength tuning from 1860 to 2090 nm *Opt. Lett.* **27** 1989–91
[14] Jackson S D 2012 Towards high-power mid-infrared emission from a fibre laser *Nat. Photon.* **6** 423–31
[15] Zhang B, Cao D, Jiao Z and Wang B 2014 All-fiberized polarized mode-locked thulium-doped fibre laser *Laser Phys. Lett.* **12** 015102
[16] Meng Y, Niang A, Guesmi K, Salhi M and Sanchez F 2014 1.61 μm high-order passive harmonic mode locking in a fiber laser based on graphene saturable absorber *Opt. Express* **22** 29921–6
[17] Agrawal G P 2013 *Nonlinear Fiber Optics* 5th edn (Amsterdam: Elsevier)